Transport Modelling of Stellarators with ASTRA

Nikolai E. Karulin

IPP 2/328 December 1994

MAX-PLANCK-INSTITUT FÜR PLASMAPHYSIK

85748 GARCHING BEI MÜNCHEN

MAX-PLANCK-INSTITUT FÜR PLASMAPHYSIK

GARCHING BEI MÜNCHEN

Transport Modelling of Stellarators with ASTRA

Nikolai E. Karulin

IPP 2/328 December 1994

Die nachstehende Arbeit wurde im Rahmen des Vertrages zwischen dem Max-Planck-Institut für Plasmaphysik und der Europäischen Atomgemeinschaft über die Zusammenarbeit auf dem Gebiet der Plasmaphysik durchgeführt.

Abstract

The transport code ASTRA (an Automatic System for Transport Analysis in a Tokamak) was developed at Kurchatov Institute for Atomic Energy, Moscow several years ago to analyse plasma transport in tokamaks. Since that time the code appeared to be a powerful tool applicable to various tasks, such as predictive transport modelling, analysis of experimental results, study of scenarios, examination of theoretical transport models. This paper deals with transport simulations fulfilled with a version of the ASTRA code extended for stellarators. Stellarator neoclassical transport models of Beidler, Kovrizhnykh, Hastings-Houlberg-Shaing and Maaßberg were included in the stellarator version of the code. The ambipolar radial electric field is calculated in all these cases self-consistently. The results for such devices as Wendelstein 7-AS and a Helias reactor are presented.

Introduction

The transport modelling in both tokamaks and stellarators deals with at least the following topics.

- Predictive modelling, which makes it possible to plan of experiments on running or future machines.
- Evaluation and analysis of experimental results, which serves for understanding of basic physical processes in the plasma.
- Examination of theoretical or empirical transport models developed analytically or numerically,its comparison to experimental data.

On tokamaks, this approach is common and has become routine now. Another situation is typical for stellarator research. A suitable tool for the analysis is not available for every experiment. Stellarator neoclassical transport is, however, more complex and sometimes it cannot be properly described theoretically owing to the complexity of magnetic configurations. That is why it is common to calculate the transport coefficients directly by solving the drift kinetic equation or from the Monte Carlo simulations. Such methods require much computer time and, because of that, are hardly suitable for fast transport analysis.

This task can be fulfilled by ASTRA provided that the transport matrix is known from theory or sophisticated numerical models. Further desirable requirement to a transport code, which ASTRA satisfy, is that the tool should be flexible, fast and clear enough to be used by a physicist.

This paper presents the results of predictive and interpretive transport simulations fulfilled with the help of the transport code ASTRA. The paper is structured as follows: in Sec.I a brief review of transport equations is given; some remarks to transport modelling in stellarators are made in Sec.II; reactor calculations are described in Sec.III; the transport simulation of the ECRH discharge of Wendelstein 7-AS is summarized in Sec.IV, conclusions are formulated in Sec.V. The appendicies provide the description of the transport model which has been typically used in the simulations, a list of new subroutines developed for stellarator applications, and the summary of the code.

I.Transport equations

The system of one-dimensional equations averaged over the toroidal magnetic surfaces is used by ASTRA when calculating the transport of energy and particles. Full description of the complete system of transport equations and of the averaging method can be found in the original paper[1]. As a rule, the code solves four balance equations (for T_e, T_i, n_e, and the poloidal magnetic flux ψ) using 4×4 transport matrix. In Gaussian units the set of equations has the following form:

[1] G. V. Pereverzev, P. N. Yushmanov et al., IPP Report 5/42, 1991

$$\frac{\partial}{\partial t}(V' n_e) \;+\; \frac{\partial}{\partial \rho}\left(V' <(\nabla\rho)^2> \Gamma_e\right) = V'\, S$$

$$\frac{3}{2}\frac{1}{\rho}(V')^{-5/3}\frac{\partial}{\partial t}(\rho(V')^{5/3} n_e T_e) \;+\; \frac{1}{V'}\frac{\partial}{\partial \rho}\left(V' <(\nabla\rho)^2> (q_e + \frac{5}{2} T_e \Gamma_e)\right) = P_e$$

$$\frac{3}{2}\frac{1}{\rho}(V')^{-5/3}\frac{\partial}{\partial t}(\rho(V')^{5/3} n_i T_i) \;+\; \frac{1}{V'}\frac{\partial}{\partial \rho}\left(V' <(\nabla\rho)^2> (q_i + \frac{5}{2} T_i \Gamma_i)\right) = P_i$$

$$\frac{2\pi B_0}{c}\frac{\rho}{V'}\sigma_{\|}\frac{\partial \psi}{\partial t} \;=\; \frac{cI^2}{8\pi^2 V'}\frac{\partial}{\partial \rho}\left(\frac{V'}{I} <(\frac{\nabla\rho}{r})^2> \frac{\partial \psi}{\partial \rho}\right) - <(\mathbf{j}_{bs} + \mathbf{j}_{ext})\mathbf{B}>\,,$$

where $q_{e,i}$ are the average electron and ion heat fluxes, $\Gamma_{e,i}$ are the average particle fluxes. All quantities in this system depend on time and on a radial variable ρ which is in turn a label of the magnetic surface. These fluxes are linked to the generalized forces via the matrix

$$\begin{vmatrix} \frac{\Gamma_e}{n_e} \\ \frac{q_e}{T_e} \\ \frac{q_i}{T_i} \\ \frac{4\pi}{c}\frac{R_0 J_B}{B_0 \rho \mu} \end{vmatrix} = - \begin{vmatrix} D_n & D_e & D_i & D_E \\ \kappa_e^n & \kappa_e & \kappa_e^i & \kappa_e^E \\ \kappa_i^n & \kappa_i^e & \kappa_i & \kappa_i^E \\ C_n & C_e & C_i & 0 \end{vmatrix} \times \begin{vmatrix} \frac{1}{n_e}\frac{\partial n_e}{\partial \rho} \\ \frac{1}{T_e}\frac{\partial T_e}{\partial \rho} \\ \frac{1}{T_i}\frac{\partial T_i}{\partial \rho} \\ \frac{cE}{B_p} \end{vmatrix} .$$

To close the system of transport equations it is necessary to determine the averages of the metric coefficients $<(\nabla\rho)^2>$, $<(\nabla\rho/r)^2>$, the volume derivative $V'(\rho) \equiv \partial V/\partial\rho$ and the current $I(\rho)$. For tokamaks a simplified moment description of the equilibrium is used for this purpose:

$$r \;=\; R_0 + \Delta(a) + a\,(cos\theta - \delta(a)\, sin^2\theta)$$

$$z \;=\; a\lambda(a)\, sin\theta\,,$$

where elongation $\lambda(a)$, triangularity $\delta(a)$ and shift $\Delta(a)$ are calculated. The electric field in the system of equations above is the longitudinal field $E_{\|}$.

For stellarators there is no simple model for MHD equilibrium at present. Instead, the metric coefficients can be incorporated as input from other codes. The last equation for the poloidal flux ψ is not solved in the stellarator case. The toroidal current density profile should be prescribed in accordance with the radial dependence of the rotational transfor-

mation. The electric field is now the radial field E_ρ and is calculated from ambipolarity of the neoclassical particle fluxes.

Sources and sinks S, P_e, and P_i in the right parts of the main system of equations contain a set of common terms. For particles there are the source terms corresponding to ions coming from cold neutrals and from a neutral beam, the sink term governed by recombination. External heating (ECR, ICR, LHW and NBI) and current drive, electron-ion Coulomb heat exchange, Ohmic heating, radiation losses, losses on cold neutrals, α-heating, etc. are all can be included in the right parts of the energy transport equations. Boundary conditions for the plasma density and temperatures can be either prescribed, or calculated from a simple built-in SOL model.

II.Transport modelling for stellarators

Transport processes in stellarators have some important features which should be taken into account when creating transport models. First of all, the neoclassical particle fluxes are not automatically ambipolar at arbitrary radial electric field. Moreover, the electric field E_r is responsible for sustaining ambipolarity, but, on the other hand, it determines the transport coefficients themselves. That is why the equations for the particle and heat fluxes become non-linear with respect to the electric field. To illustrate this fact, we write out the expressions for the particle and heat fluxes explicitly in the form[2]:

$$\Gamma_j = -D_1 n_j \left(\frac{n_j'}{n_j} - \frac{q_j E_r}{T_j} + \left(\frac{D_2}{D_1} - \frac{3}{2} \right) \frac{T_j'}{T_j} \right)$$

$$Q_j = -D_2 n_j T_j \left(\frac{n_j'}{n_j} - \frac{q_j E_r}{T_j} + \left(\frac{D_3}{D_2} - \frac{3}{2} \right) \frac{T_j'}{T_j} \right)$$

where

$$D_n(E_r) = \frac{2}{\sqrt{\pi}} \int_0^\infty dx_j \, x_j^{(2n-1)/2} D(x_j) e^{-x_j} \, ,$$

$D(x_j)$ is the monoenergetic diffusion coefficient and $x_j = m_j v^2/(2T_j)$ is the dimensionless particle's energy.

From these expressions one finds that the neoclassical diffusion coefficient is given by $D_n = D_1(E_r)$, and the thermal conductivity is given by $\chi_{nc} = D_3(E_r) - 3/2 \, D_2(E_r)$. It is seen immediately that the transport matrix is non-diagonal. To find proper transport coefficients means also to calculate the self-consistent electric field. The way of finding the radial electric field is actually not obvious and needs special treatment for different regimes of collisionality.

Another problem concerns metric properties of the stellarator magnetic configurations. This problem is partially resolved in ASTRA for tokamaks by solving equilibrium problem with the help of the momentum description. A similar fast procedure for the three dimensional stellarator equilibrium is not developed yet. On the other hand, the magnetic surfaces for stellarators, as a rule, are calculated also in space coordinates (cartesian or cylindrical) after solving the general equilibrium problem. Hence, it is natural to use such representations for computing the average values of metric coefficients $< (\nabla\rho)^2 >$,

[2] W. Lotz, J. Nührenberg, Physics of Fluids, **31**, 1988, p.2984

$< (\nabla\rho/r)^2 >$ needed for the transport equations above. The difference from the tokamak case is that these values are not calculated by ASTRA, but are incorporated by the code from the external equilibrium code.

The balance equation for the poloidal flux, as was mentioned above, is not solved for stellarators. In order to obtain the proper profile of the stellarator rotational transformation ι, the following expression governing the longitudinal current density should be used

$$j = \frac{c}{8\pi^2}\frac{R}{V'}\frac{\partial}{\partial\rho}\left(V' < (\nabla\rho/r)^2 > \frac{\partial\psi}{\partial\rho}\right) \approx \frac{cB_0}{4\pi R}\frac{1}{\rho}\frac{\partial}{\partial\rho}(\iota\rho^2),$$

where the profile $\iota(\rho)$ is given. This current is not included in the Ohmic heating term.

III.Helias reactor

As a reference case for the subsequent simulation a stellarator reactor of Helias type with the main parameters presented in Table 1 was taken. This concept is under consideration at IPP for several years[3].

Table 1: Reference parameters of the Helias reactor

Major radius, $R\,[m]$	22
Average plasma radius, $a\,[m]$	1.75
Magnetic field, $B\,[T]$	5
Rotational transform, ι	0.85–0.96
Peak plasma density, $n\,[10^{19}m^{-3}]$	4.0
Line-averaged plasma density, $\bar{n}\,[10^{19}m^{-3}]$	2.98

The reference magnetic configuration called HS5V10NR was obtained by J.Kißlinger and reproduces in general the scaled up one of Wendelstein 7-X. This configuration is formed by a five-period magnetic coil system with ten non-planar coils in every toroidal period. All sets of ten coils are equivalent. Fourier components of the magnetic field strength B expressed in flux coordinates

$$\frac{B}{B_0} = 1 + \sum_{m,l} C_{m,l}\, cos\, m\theta\, cos\, lp\phi + \sum_{m,l} S_{m,l}\, sin\, m\theta\, sin\, lp\phi$$

are plotted in Figure 1. The only essential difference from W 7-X is the greater modular ripple term $C_{0,1}$.

[3] C.D.Beidler, E.Harmeyer, J.Kißlinger, I.Ott, F.Rau, H.Wobig. Report IPP 2/318, 1993

The transport model included neoclassical coefficients obtained by C.Beidler[4] (see also Appendix A below). It is well known from experiments that behavior of plasma electrons is not purely neoclassical, that is why the electron thermal conductivity was taken as a sum of neoclassical and anomalous terms $\chi_e = \chi_{e,nc} + \chi_a$. The anomalous part χ_a was taken in the form which fits the L-mode confinement in the ASDEX tokamak[5] extrapolated to a Helias reactor, where a plateau-like scaling ($\propto RB^2$) has been assumed

$$\chi_{L-mode}[m^2/s] = 1.5 \frac{1.6}{R[m]} \frac{2.2}{B[T]}^2 \frac{T_e^{3/2}[keV^{3/2}]}{(1.1-(r/a)^2)^4}.$$

The ions were, in turn, assumed to be neoclassical.

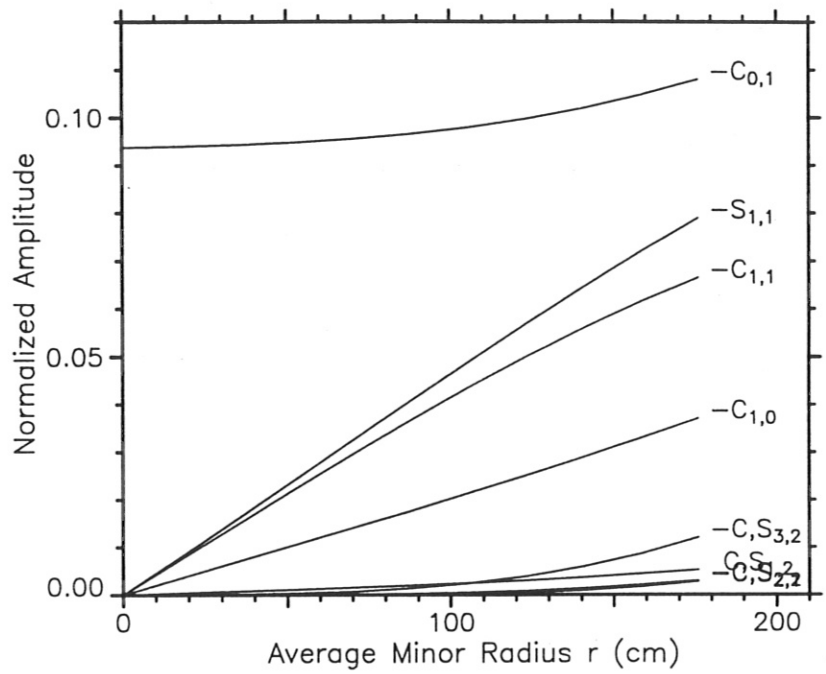

Figure 1: Main Fourier harmonics of the magnetic configuration of the reference Helias reactor.

The plasma electrons were heated by ECR power deposited on the axis of the plasma column with the parabolic profile $P_{ECR} \propto (1-(\rho/a)^{100})$ and the ions got their energy from Coulomb interaction with the electrons. Thermonuclear power from $3.5MeV$ alpha particles was distributed between the electrons and ions. The heat losses were due to bremsstrahlung, synchrotron radiation and radiation losses on impurities. Since the content of impurities in the reactor is not known, the corresponding losses were approximated by a prescribed profile function with a maximum near the plasma edge. Up to 50% of the heating power $Q_\alpha + Q_{ECR}$ was lost through the electron channel because of that model loss.

[4] C.Beidler In proceedings of the IAEA Technical Committee Meeting on Stellarators and other Helical Confinement Systems, Germany 10-14 May 1993, IAEA Vienna, 1993, p.138

[5] K.Lackner et al., Plasma Physics and Controlled Fusion **31**, No.10, (1989), p.1626

In order to heat up plasmas at such high plasma densities by ECR power, an X-mode wave on the fundamental frequency of $140GHz$ should be used. This wave has a high cut-off density of $4.8 \cdot 10^{20} m^{-3}$ but should be injected into the torus from the high-field side. Estimated absorption is good at the electron temperatures $T_e > 6keV$.

The plasma density with a relatively flat profile was fixed for simplicity. Fuel dilution through cold alpha particles decreases the effective plasma density $n_d = n_t = n_e - 2n_{He}$. Plasma quasi-neutrality was, therefore, sustained.

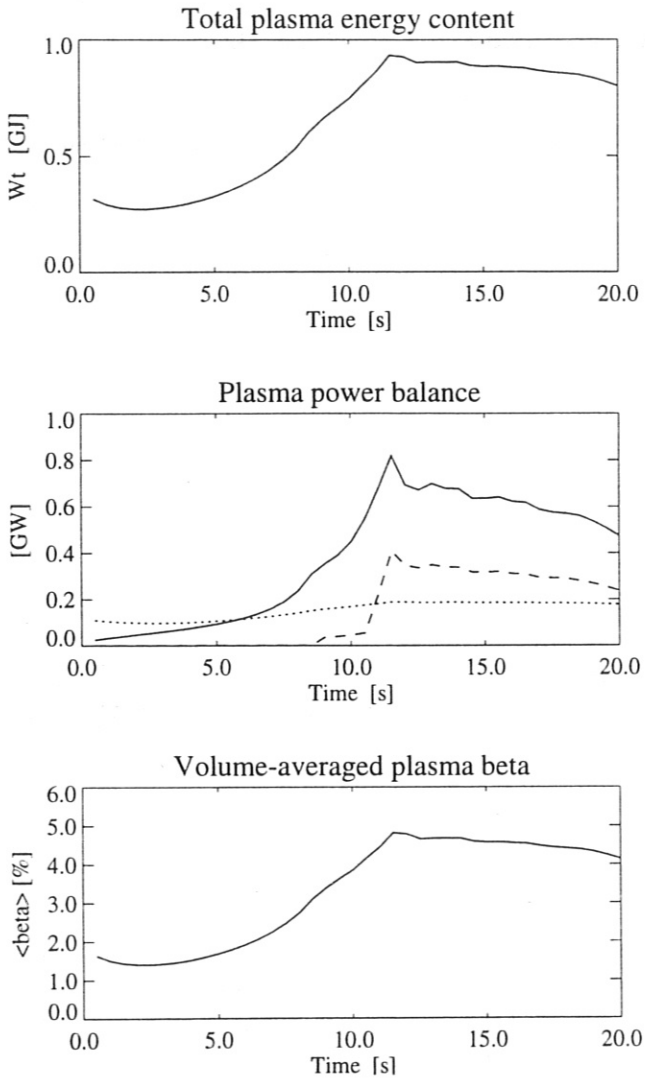

Figure 2: Time development of plasma parameters in the reference Helias reactor. b) solid curve is the thermonuclear power in alpha particles Q_α; broken curve is the total edge radiation Q_{imp}; dotted curve are the bremsstrahlung losses Q_{br}.

Time development of the main plasma integral parameters is plotted in Figure 2. The plasma with the initial peak temperatures $T_e(0) = T_i(0) = 3.5keV$ was heated by $50MW$

ECR power (on-axis deposition).

After a relatively long starting phase of about 7 seconds the plasma becomes hot enough, so that the thermonuclear power released in α-particles begins to heat it up more intensively. It seems that $50MW$ of ECR power is the lowest value of power needed to heat up the reactor to ignition, which corresponds to the results of Ref. 3.

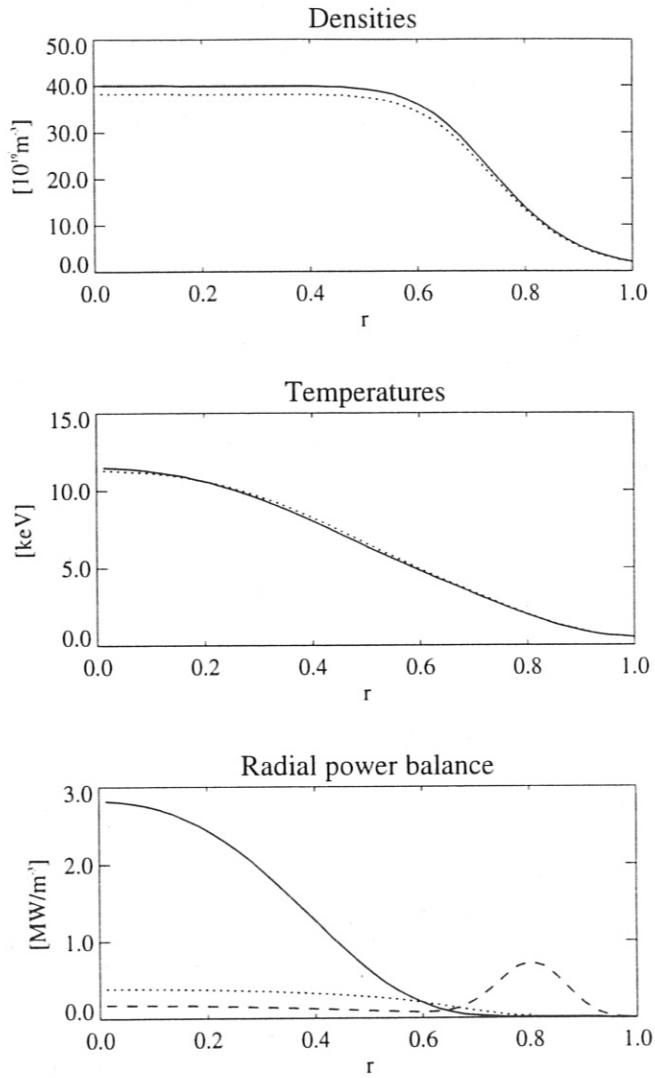

Figure 3: Operational point at $t = 16.5s$. a) Profiles of the electron (solid curve) and ion densities. b) Electron (solid curve) and ion temperatures. c) Alpha particle heating power P_α (solid curve); bremsstrahlung losses P_{br} (dotted curve); model radiation losses on impurities P_{imp}. Parameters of the plasma: total energy content $W_t = 0.878GJ$; fraction of α-particles $f_\alpha \equiv n_{He}/n_e = 5\%$; peak plasma beta $\beta(0) = 14.3\%$; volume-averaged beta $<\beta>= 4.54\%$; α-power $Q_\alpha = 0.62GW$; bremsstrahlung radiation $Q_{br} = 0.19GW$; impurity radiation $Q_{imp} = 0.31GW$, energy confinement time $\tau_E = 2.01s$ ($\tau_{LG} = 3.37s$, $\tau_{LHD} = 2.03s$, $\tau_{g-B} = 1.77s$).

The steady state is reached at the moment t=16.5s. Figure 3 presents the plasma

densities, temperatures and radial power balance.

It is well known that D-T reaction rate increases with the ion temperature, $<\sigma v>_{dt} \propto T^n$, where n is greater than 2. That is why the operational point of a thermonuclear reactor should be stabilized to avoid thermal instability and run-off in the region of extremely high temperatures and plasma betas. The thermonuclear thermal instability in tokamaks would lead to disruptions. In the simulation for the Helias reactor the stabilization was achieved by means of soft deterioration of transport properties at values of the volume-averaged beta above $<\beta>_{lim}= 4.5\%$. This quantity seems to reflect a threshold for onset of ballooning instabilities in the stellarator plasmas. The exact mechanism of influence of this MHD-activity on the discharge was not, however, investigated within the scope of this work.

To illustrate the transport properties of the reactor we plotted in Figure 4 the thermal conductivities and ambipolar electric field.

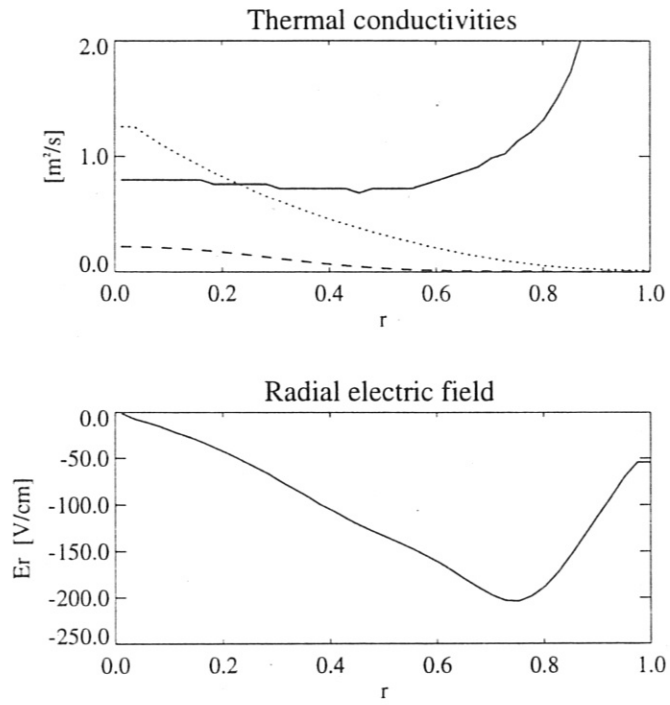

Figure 4: Helias reactor steady state, t=16.5s. a)Electron thermal conductivity $\chi_e = \chi_{e,nc} + \chi_a$ (solid curve); ion thermal conductivity χ_i (dotted curve); neoclassical part $\chi_{e,nc}$ of the electron thermal conductivity. b)Ambipolar radial electric field.

It is seen from Figure 4 that the ion and anomalous electron transport compete in the inner region of the plasma column, whereas the electron heat transport strongly dominates in the outer region. The neoclassical part of the electron transport being sufficiently smaller, than the anomalous one, contributes only in the inner region. It should be mentioned that the last statement is correct as long as the experimentally observed anomalous behavior remains valid also for the reactor plasmas.

It would be interesting to know, how the chosen transport model fits the well known scalings for the global energy confinement time τ_E. Figure 5 demonstrates the results of this comparison. Lackner-Gottardi scaling gives more encouraging values than the LHD and gyro-Bohm scalings for the Helias reactor plasma parameters. The calculated global energy confinement time τ_E which is, however, correctly defined only for stationary plasmas (at times greater than about $12s$ in our case) agrees almost exactly with the LHD-scaling. Since the anomalous electron thermal conductivity has been derived in the simulation from the Lackner-Gottardi model, one could expect that τ_E should be close to τ_{LG}. Since this is not the case, it means that not only the anomalous electron transport, but also neoclassical ion transport determines transport properties of the Helias reactor. If the neoclassical transport could be reduced, the constraints on the minimal reactor size, magnetic field strength, required heating power and allowable fuel dilution could be relaxed.

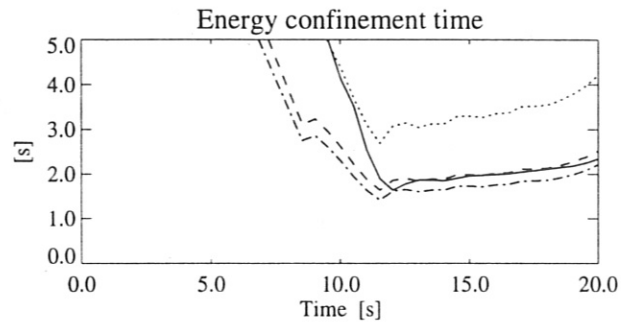

Figure 5: Global energy confinement time τ_E (solid curve), Lackner-Gottardi scaling for stellarators (dotted curve), LHD-scaling (broken curve) and gyro-Bohm scaling as functions of time.

From the technical point of view, it would be desirable to consider a reactor with a lower main magnetic field B. First, the forces on the coils and support structure scale as B^2 and, second, the maximum field strength on the superconducting coils determines the choice of the superconductor material. The material with a good experimental data base and manufacturing experience $NbTi$ has lower critical magnetic field than the advanced material Nb_3Sn. The mentioned reactor concept[3] is oriented mainly on state-of-the-art technical solutions. Because of that, a reactor with a reduced to $4.7T$ magnetic field was simulated as well.

The scenario of the start-up was the same as in the reference case, except for the ECR heating power which had to be increased up to $60MW$. The soft MHD limit was increased to $<\beta>_{lim}= 5\%$. In the low-field case, the allowable fraction of α-particles $f_\alpha \equiv n_{He}/n_e$ must not be higher than 2%.

To sustain this low value, the diffusion coefficient of cold helium should be by a factor of 1.5 larger than the thermal conductivity of the background ions χ_i.

The summary of the main operational parameters corresponding to the reference and low-field case are summarized in Table 2. If the magnetic field is lower than $4.7T$, it seems to be impossible to achieve a steady state at reasonable plasma betas without improving transport (H-mode) or increasing the reactor size.

Table 2: Operational parameters of the Helias reactor

	$B = 5T$ (reference)	$B = 4.7T$ (low-field)
Fusion power, $[GW]$	3.09	3.05
α-Power, $[GW]$	0.618	0.610
Plasma energy, $[GJ]$	0.878	0.852
Average beta, [%]	4.54	4.98
Peak beta, [%]	14.3	15.8
Helium content, [%]	5	2
Ion temperature $T_i(0)$, $[keV]$	11.3	10.9
Energy confinement time $\hat{\tau}_E$, $[s]$	2.01	1.93
τ_{LG}, $[s]$	3.37	3.22
τ_{LHD}, $[s]$	2.03	1.94
τ_{g-B}, $[s]$	1.77	1.69

IV. Wendelstein 7-AS

Stellarator W 7-AS is a modular partially optimized stellarator with five periods of main coils and a set of additional coils capable to vary to some extent its magnetic configuration. Fourier spectrum of the magnetic field of this machine contains more harmonics than the optimized Helias reactor and, therefore, this device is difficult to be described by the analytical neoclassical transport theory. Nevertheless, the theory predicts functional dependencies on collisionality and ambipolar electric field, which can be summarized in the formulation for the monoenergetic diffusion coefficient[4] (see also Appendix A):

$$D^{-1} = D_{1/\nu}^{-1} + D_{\sqrt{\nu}}^{-1} + D_{\nu}^{-1} \ ,$$

where $D_{1/\nu} \propto \nu^{-1}$, $D_{\sqrt{\nu}} \propto \sqrt{\nu} \ / \ |\Omega_E|^{3/2}$, $D_{\nu} \propto \nu/\Omega_E^2$, ν is the collisional frequency and $\Omega_E = E_r/rB$ is the $\mathbf{E} \times \mathbf{B}$ precession frequency.

Recently, H.Maaßberg[6] made use of the functional dependence given by the theory to obtain numerically the neoclassical transport coefficients for W 7-AS. The fits were done with the help of the DKES code which solves the monoenergetic drift kinetic equation for the real magnetic field.

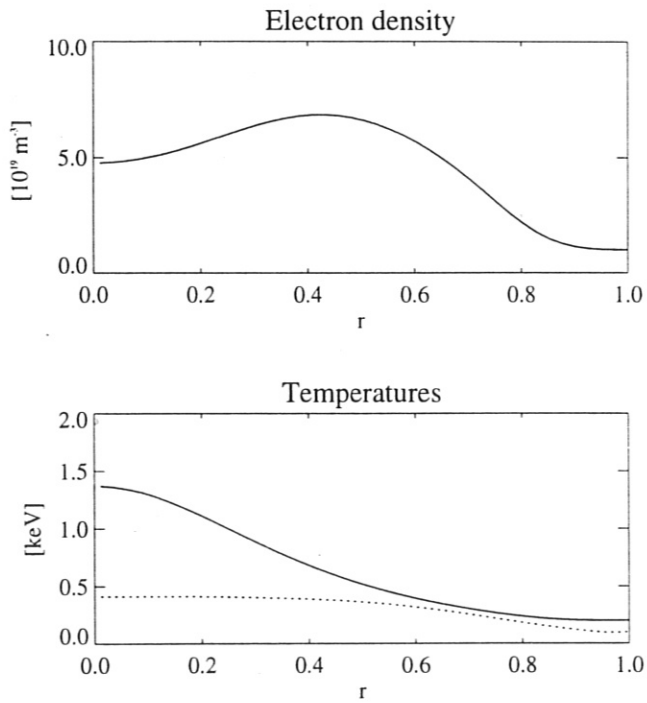

Figure 6: Simulation of the shot number 28531 of W 7-AS. Discharge parameters: $B = 2.54\,T$, $\iota(a) = 0.345$, $P_{ECR} = 0.833\,MW$ (on-axis deposition). a)Electron density; b)Electron (solid) and ion (dotted) temperatures.

Although the work is still in progress, we present below the first results of the simulation

[6] C.D.Beidler, W.Lotz, H.Maaßberg Neoclassical Transport Scalings for Stellarators in the Long-mean-free-path Regime, Proc. of the 21-th European Conf. on Contr. Fusion and Plasma Physics, Montpellier, France, 1994, in press

of a typical discharge. The shot number 28531 has been simulated using the transport model referred to above. It was a discharge with a moderate density of $\bar{n}_e = 4.7{\cdot}10^{19} m^{-3}$, relatively high ECR heating power of $P_{ECRH} = 0.833\ MW$ and with a slightly hollow density profile.

To simulate this discharge, the equation for the electron density has also been solved. To give an idea how the model for the density looked like in this simulation, we write the expression for the particle flux explicitly:

$$\Gamma_e = -D_n n' - D_e \frac{n_e}{T_e} T_e' - D_E\, n_e \frac{E_r}{eT_e}\ ,$$

where E_r is the radial electric field. The coefficients D_e and D_E were neoclassical, whereas D_n was taken as a sum of the neoclassical and anomalous terms $D_n = D_{n,nc} + D_{n,an}$. The anomalous part was in turn determined as $D_{n,an} = f\chi_{L-mode}$ with the numerical factor f of several percents. The ion density was taken to be equal to that of electrons.

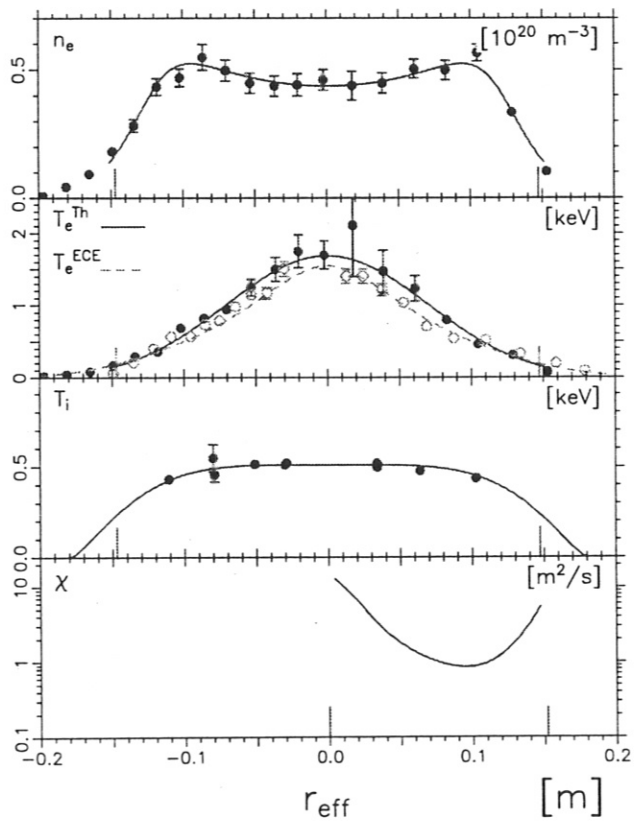

Figure 7: Experimental profiles from the shot number 28531 of W 7-AS (kindly presented by G.Kühner).

Radial distribution of the ions appearing in the plasma as a result of ionization, as well as the corresponding power losses of the bulk ions and electrons, were calculated

using a slab model for neutrals. Density of neutrals on the plasma edge served as input for the calculation of the particle source in the plasma column. Apart from the particle transport, ionization and recombination of the neutrals were responsible for building the plasma density profile.

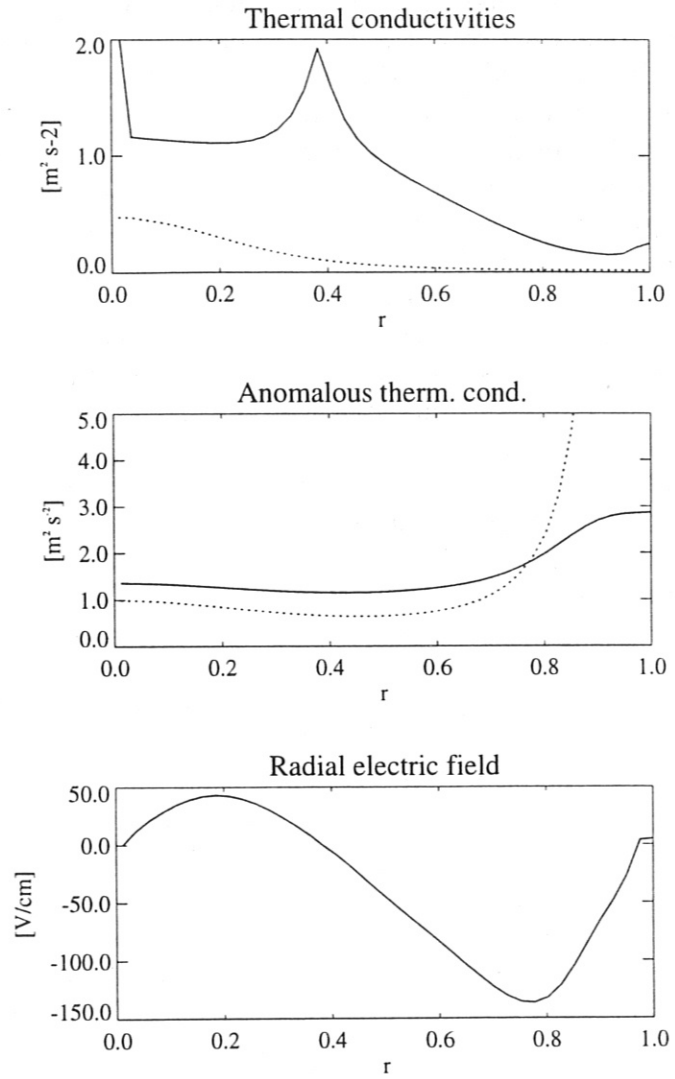

Figure 8: Transport coefficients of the shot number 28531 of W 7-AS. a)Ion (solid) and electron neoclassical thermal conductivities; b)Anomalous electron thermal conductivities. Dotted curve is the ASDEX L-mode-like scaling, χ_{L-mode} (see previous Section), which was used for the simulation. Solid curve is W 7-AS scaling $\chi_{e,an}[m^2/s] = 186\, B^{-0.954}[T]\, n_e^{-0.477}[cm^{-3}]\, P_{ECR}[W]\, \epsilon_a^{-0.684}$ plotted for comparison. c)Ambipolar radial electric field

As a reference, we present in Figure 7 the measured profiles of the electron density and of the both temperatures. It can be seen from comparing the Figures 6 and 7 that the density profile has been satisfactorily reproduced in the simulation. The fine structure

of the profiles near the edge is, however, different owing to the fact that there is always plasma behind the limiter, and this effect has not been simulated. The calculated electron temperature on the axis is lower than that obtained from Thomson scattering but close to the ECE measurements. The ion temperature is lower than the measured one as well, but its value depends strongly on the flow of neutrals from the edge, which was not known at the time of simulation. The total heat losses on neutrals was $Q_{cx} = 177\ kW$.

The question often arises, what sort of transport dominates: electron or ion. In Figure 8 the thermal conductivities derived from the transport model are plotted. It is seen, first of all, that the ion heat transport is comparable with the anomalous electron one, or the former even dominates. The peak of the ion thermal conductivity at $r/a \approx 0.4$ is owing to the radial electric field which is close to zero at that radius. It is also an indication that the ions are not in $1/\nu$ regime, because in this regime the ripple transport is independent of the electric field. The neoclassical electron heat transport is smaller than the anomalous part of the electron transport as expected.

Both scalings for the anomalous electron thermal conductivity give similar profiles, the absolute values of the ASDEX-L scaling being, however, lower in the plasma core than the W 7-AS scaling. The outer plasma region can not be described by W 7-AS scaling, since it gives too small values for χ_e.

An obvious discrepancy exists between the curve for the electron thermal conductivity in Figure 7 and the similar curves in Figure 8. The values of the electron thermal conductivity χ_e at $r/a < 4cm$ derived from the experiment (Figure 7) are too large and are not consistent with the measured electron temperature T_e. Even with the smaller heat transport, given by the transport model used in the simulation, the peak electron temperatures of above $1.5keV$ could not be achieved. This difference could be caused by taking into account only diagonal terms in the transport matrix when analyzing experimental profiles. Whereas the non-diagonal terms, including the one proportional to the radial electric field, contribute in the heat fluxes as well.

V.Conclusions

The ASTRA code extended for stellarator applications appears to be an adequate tool to perform predictive and interpretive transport analysis in non-axisymmetric geometry which requires the use of the full transport matrix. Calculation of the self-consistent radial electric field is fulfilled in many cases on the "real" time scale which makes it possible to simulate various heating scenarios. Appropriate transport models describing experimental discharges can be easily incorporated in the code.

The simulation of scenarios for the Helias reactor confirms the main results of the earlier zero dimensional study. The $22\ m$ reactor with the magnetic field of $B = 5\ T$ reaches ignition at reasonable values of the plasma beta (see Table 2 above) without enhanced confinement (H-mode). The power of about 600 MW released in thermonuclear alpha particles seems to be a universal threshold for ignition in such a reactor. Changing the plasma density or helium content has almost no influence on that criterion. Reduction of the neoclassical ion transport or of the anomalous electron transport would eventually relax requirements on the reactor size, magnetic field, heating power or helium extraction.

The global energy confinement agrees to the LHD-scaling $\tau_E \approx \tau_{LHD} \approx 2\,s$ where that

scaling is taken with the isotope factor of 2.5. If the isotope effect is excluded from the scalings, the global energy confinement time τ_E fits the Lackner-Gottardi scaling.

A reactor with a smaller magnetic field of 4.7 T operates at higher volume-averaged beta of 5% and lower allowable fraction of cold α-particles ($f_\alpha = 2\%$.

One of the high-power ECRH discharges of Wendelstein 7-AS has been modelled using the neoclassical transport matrix created by H.Maaßberg with the help of the DKES code. The plasma density profile was reproduced satisfactorily, whereas the peak electron temperature is lower than that obtained by Thomson scattering. The neoclassical ion thermal conductivity given by the model is comparable with the anomalous electron thermal conductivity. Both empirical formulas of the anomalous electron thermal conductivity $\chi_{e,an}$ in the form of the ASDEX L-mode and of W 7-AS scaling give comparable values. The W 7-AS scaling cannot properly describe the outer region of the plasma column. In order to evaluate the plasma transport analyzing the experimental profiles, it seems to be indispensible to use the full transport matrix.

Calculation of the ambipolar electric field in the regimes of low collisionality needs special attention. The electron root arising in the plasma region adjacent to the magnetic axis, whereas in the rest plasma the ion root still exists, leads to physical and numerical difficulties.

Acknowledgements

I would like to express my gratitude to Dr.H.Wobig who has made it possible for me to carry out this work at IPP.

I specially thank Prof.G.V.Pereverzev, who is one of the authors of ASTRA, for his continuous help with the code.

I would like to thank Dr.H.Maaßberg for the contribution he made and many useful discussions.

I wish to thank the members of the group, in which I worked, Drs. C.Beidler, J.Kißlinger, F.Rau for fruitful cooperation.

Appendix A. Stellarator transport model used in the simulations

The transport models based on the theory developed by C.Beidler[4] have been most frequently used in the simulations. A list of corresponding formulas for the monoenergetic diffusion coefficient is presented below.

The ripple diffusion coefficient can be expressed as follows:

$$\frac{1}{D_h} = \frac{1}{D_{1/\nu}} + \frac{1}{D_{\sqrt{\nu}}} + \frac{1}{D_\nu},$$

where the three particular coefficients reflect transport properties for different values of collisionality.

The diffusion coefficient for high collision frequencies $D_{1/\nu}$ is

$$D_{1/\nu} = \frac{4}{9\pi}(2\epsilon_{eff})^{3/2}\frac{v_d^2}{\nu_j},$$

where v_d is the radial drift velocity given by

$$v_d = \frac{eT_j}{q_j B_0 R_0} x_j,$$

and $x_j = m_j v^2/(2eT_j) = v^2/v_j^2$, is the dimensionless particle velocity, ϵ_{eff} is the so-called effective ripple which characterizes transport properties of the magnetic configuration in $1/\nu$ collisionality regime where $\nu_{eff} \gg \Omega_E$.

In the intermediate range of collision frequencies the diffusion coefficient is

$$D_{\sqrt{\nu}} = \frac{4}{9\pi}\alpha_{\sqrt{\nu}}\left(v_d\frac{C_{0,1}}{\epsilon_t}\right)^2\frac{\nu_j^{1/2}}{\mid \Omega_E \mid^{3/2}},$$

with a fitting factor $\alpha_{\sqrt{\nu}}$ and $\epsilon_t = \rho/a$.

For low collision frequencies where $\nu_{eff} \ll \Omega_E$, D is given by

$$D_\nu = \frac{\alpha_\nu}{9\pi}\left(v_d\frac{C_{0,1}}{\epsilon_t}\right)^2\frac{\nu_j}{\Omega_E^2\mathcal{F}_{bl}},$$

with a fitting factor α_ν and where $\mathcal{F}_{bl} = \sqrt{C_{0,1} + 2\epsilon_h} - \sqrt{2\epsilon_h}$, ϵ_h is the helical ripple. The factors $\alpha_{\sqrt{\nu}}$ and α_ν can be chosen to fit Monte Carlo or DKES calculations.

The axially symmetric part of the particle transport is described by the following coefficients:

$$D_a = (D_{bp}^{3/2} + D_{ps}^{3/2})^{2/3},$$

where

$$D_{bp} = \frac{D_b D_p}{D_b + D_p},$$

and the diffusion coefficient in the banana regime D_b is

$$D_b = \frac{\mid C_{0,1} \mid}{\epsilon_t^2\mathcal{F}_{bl}}\frac{v_d R_0}{\Omega_t^2}\nu_j,$$

in plateau regime it is

$$D_p = \frac{1}{3}\left(\frac{C_{0,1}}{\epsilon_t}\right)^2 \frac{v_d v x_j^{1/2}}{\Omega t} ,$$

and in Pfirsch–Schlüter regime it is

$$D_{ps} = \frac{7}{5}\left(\frac{C_{0,1}}{\epsilon_t}\right)^2 \frac{v_d R_0}{\Omega t^2}\nu_j ,$$

where $\Omega = qB_0/m$ is the Larmour frequency.

The resulting monoenergetic diffusion coefficient takes now the form of a sum of the axisymmetric (tokamak-like) and helical terms.

$$D = D_h + D_a .$$

The expressions for the elements of the transport matrix derived from the monoenergetic transport coefficient, as well as the expressions for the particle and heat fluxes, one can find in Sec.II above.

Appendix B. Transport Code Summary

Name:	ASTRA
Authors:	G. Pereverzev, P. Yushmanov, A. Polevoi, A. Dnestrovkii, N. Karulin et al.
Transport equations:	Time dependent, for n_e, T_e, T_i, ψ, α-particles
Transport model:	User's choice
Magnetic configuration:	Fixed boundary momentum equilibrium for tokamaks, metric coefficients from an external equilibrium code for stellarators
Electric field	Self-consistent ambipolar radial electric field for stellarators
Neutrals:	Kinetic description in a slab model
Heating and CD:	NBI (pencil beam, instantaneous deposition) ECR (beam tracing) LHW (beam tracing) ICR (under development)
Sawteeth:	Reconnection model or enhanced transport
α-heating:	Local, instantaneous deposition
Impurities:	Coronal equilibrium with some corrections or prescribed profiles
Boundary conditions:	Prescribed values/fluxes or 0-D SOL model
Stability:	Tearing modes (Δ' analysis) Ideal MHD stability analysis for specified time slices
Run time:	Basic version: $\approx 0.1s/t$-step
Computing features:	Real time, interactive or batch mode with postrun analysis
Computer language:	Fortran, C, C-shell
Operating system:	At present, DOS, UNIX

Appendix C. List of stellarator transport subroutines for ASTRA

HELT7: transport model for optimized stellarators of Helias type based on the neo-classical theory developed by C.Beidler.

HHS2: transport model based on Hastings-Houlberg-Shaing[7] theory.

FITS: transport model based on fits made by H.Maaßberg with DKES.

HELHSX: transport model for optimized helically symmetric stellarators (HSX) based on C.Beidler's model.

KOVR: transport model based on Kovrizhnykh[8] theory.

[7] D.E.Hastings, W.A.Houlberg, K.C.Shaing, Nucl. Fusion, **25**, 1985, p.445
[8] L.M.Kovrizhnykh, Nucl. Fusion **24**, 1984, p.435